ELSEVIER

Nonmonotonic dose dependence of OSL intensity due to competition during irradiation and readout

V. Pagonis[a], R. Chen[b,*,1], J.L. Lawless[c]

[a]*Physics Department, McDaniel College, Westminster, MD 21157, USA*
[b]*School of Physics, University of New South Wales, Sydney, NSW 2052, Australia*
[c]*Redwood Scientific Incorporated, Pacifica, CA, USA*

Abstract

The nonmonotonic dose dependence of thermoluminescence has been observed in several materials; a recent publication (Lawless, J.L., Chen, R., Lo, D., Pagonis, V., 2005. A model for non-monotonic dose dependence of thermoluminescence (TL). J. Phys. Condens. Matter 17, 737–753.) gave a theoretical account based on competition between trapping states or recombination centers during the excitation and/or readout stages. A similar effect has been observed in the optically stimulated luminescence (OSL) of some materials such as quartz and Al_2O_3:C (e.g., Yukihara, E.G., Whitley, V.H., McKeever, S.W.S., Akselrod, A.E., Akselrod, M.S., 2004a. Effect of high-dose irradiation on the optically stimulated luminescence of Al_2O_3:C. Radiat. Meas. 38, 317–330; Yukihara, E.G., Gaza, R., McKeever, S.W.S., Soares, C.G., 2004b. Optically stimulated luminescence and thermoluminescence efficiencies for high-energy heavy charged particle irradiation in Al_2O_3:C. Radiat. Meas. 38, 59–70.). The model of competition has now been developed to explain the nonmonotonic dose dependence of OSL. A distinction is made between two cases. In one, the competition during excitation causes the filling of the relevant radiative center to be nonmonotonic with the dose, and as a result, the OSL intensity behaves in a similar way. This can take place with a "minimal" model including one trapping state and two kinds of recombination centers, one radiative and the other nonradiative. In the other case, all the relevant concentrations increase monotonically with the dose, and the nonmonotonic dose dependence of the OSL signal is mainly due to competition in the readout stage. In this case, it appears that the requirement for nonmonotonic dose dependence is a system with two trapping states and two kinds of recombination centers.
© 2006 Elsevier Ltd. All rights reserved.

1. Introduction

Optically stimulated luminescence (OSL), also termed photo-stimulated luminescence (PSL) or, sometimes, radiophotoluminescence (RPL) is the effect in which a solid sample is first irradiated by some ionizing radiation such as α, β, γ-rays, X-rays or heavy particles and then illuminated by stimulating light, thus yielding an emission of measurable light. The emitted light is mainly the result of the dose absorbed during the initial irradiation whereas the stimulating light serves as a trigger to release the absorbed energy. Usually, the stimulating light has longer wavelength (lower photon energy) than the emitted light. However, the opposite may also take place. In this case one has to make sure that the emitted light is related to the initial excitation dose and is not merely a directly excited photoluminescence. The dependence of the OSL on the excitation dose from preceding radiation is usually an increasing function that ideally starts linearly and then goes sublinear when the OSL approaches a saturation value. OSL is closely associated with the effect of thermoluminescence (TL), the effect of emission of light during the heating of the sample following a similar excitation by ionizing irradiation. In several materials, the dose dependence function of TL has been observed to increase at low doses, reach a maximum at a certain dose, and decline at higher doses, sometimes leveling off at a certain dose. Some authors ascribed the effect to radiation damage in the sample. A review of the experimental evidence of this effect in various materials has been given by Lawless et al.

---

* Corresponding author. Tel.: +972 364 084 26; fax: +972 995 612 13.
E-mail address: chenr@tau.ac.il (R. Chen).
[1] Permanent address: School of Physics and Astronomy, Raymond and Beverly Sackler Faculty of Exact Sciences, Tel-Aviv University, Tel-Aviv 69978, Israel.

(2005). Chen et al. (2006) and Lawless et al. (2005) gave a theoretical account, which explains the nonmonotonic dose dependence as being the result of competition between transitions into different trapping states during the excitation stage, the readout stage, or both.

In the case of competition during excitation one would expect the results to be very similar whether read-out is carried out optically or thermally, since there is practically no competition during the read-out stage. Indeed it is found that the results in the case of competition during excitation are identical for OSL and TL, and the nonmonotonic behavior is the same as what has been reported in Lawless et al. (2005). In the case of competition during readout one would expect some differences between the cases of thermal and optical stimulation because of the complexity of the model. Furthermore, one of the goals of this paper is to examine how the model can be applied to Al$_2$O$_3$:C.

In a number of papers, a similar nonmonotonic dose dependence of OSL has been reported. Schulman et al. (1957) described the changes in photoluminescence due to prior γ-excitation in organic solids. In naphthalene, the dependence of 464 nm emission stimulated by 365 nm UV light depended nonlinearly on the γ-excitation dose, reaching a maximum at ∼ 10^5 Gy and decreasing at higher doses. Freytag (1971) and later Tesch (1983) and Böhm et al. (1984) described the γ-dose dependence of silver-activated phosphor glass, which is being used for dose measurements. The visible orange light stimulated by 365 nm UV light increased nearly linearly with the γ-dose between 10^{-2} and 10^2 Gy, reached a maximum at ∼ 3 × 10^3 Gy and declined at higher doses up to 10^8 Gy. The signal size was then reduced by nearly 3 orders of magnitude in the range between 3 × 10^3 and 10^8 Gy. The strict linearity with the dose between 10^{-2} and 50 Gy enables the evaluation of the dose in this region. Freytag (1971) has pointed out that the region of decreasing RPL could also be used for dose measurements provided a well-determined calibration curve is available. Zeneli et al. (1996) have further studied the behavior of radiophotoluminescent glasses which, as they report, is being used for high-level dosimetry around high-energy particle accelerators. These authors study the light emission by 365 nm stimulation following γ-irradiation. The γ-dose dependence was a nearly linear function between 10^{-1} and 10^2 Gy, reached a maximum at ∼ 10^3 Gy and declined substantially at doses up to 10^6 Gy at all the temperatures used, namely, 4.6, 77 and 300 K. The authors ascribed the decline to the self-absorption of the luminescent light. Bloom et al. (2003) studied pulsed OSL (POSL) in Al$_2$O$_3$ single crystals and reported a small decline of POSL at β doses above ∼ 10 Gy. Yukihara et al. (2004a, b) reported the effect in β-irradiated Al$_2$O$_3$:C. Both integrated CW-OSL and initial CW-OSL were found to reach a maximum at ∼ 30 Gy of β excitation, the effect being somewhat stronger in the latter than in the former. In parallel, TL measurements revealed a maximum in the dose dependence at about the same dose.

In the present work, we use models similar to those previously employed by Lawless et al. (2005) for the study of the nonmonotonic effect in TL, to explain the analogous effect in OSL.

2. The model

In a manner similar to the situation in the nonmonotonic dose dependence of TL, the minimal model which can explain the effect is given by an energy level diagram with two kinds of recombination centers and one trapping state. Certain dose dependence behavior requires, however, a system with two trapping states and two kinds of recombination centers; this is shown in Fig. 1. This energy level scheme is practically the same as that given by Lawless et al. (2005), except that the stimulation is optical rather than thermal. Of course, when the sub-model with one trapping state and two kinds of recombination center is considered, the competing trapping state N_2 is disregarded, and the active trapping state is denoted by N. The set of simultaneous differential equations governing the process during excitation in the case where two kinds of centers but only one trapping state exist is

$$\frac{\mathrm{d}m_1}{\mathrm{d}t} = -A_{m1}m_1 n_\mathrm{c} + B_1(M_1 - m_1)n_\mathrm{v}, \tag{1}$$

$$\frac{\mathrm{d}m_2}{\mathrm{d}t} = -A_{m2}m_2 n_\mathrm{c} + B_2(M_2 - m_2)n_\mathrm{v}, \tag{2}$$

$$\frac{\mathrm{d}n}{\mathrm{d}t} = A_n(N - n)n_\mathrm{c}, \tag{3}$$

$$\frac{\mathrm{d}n_\mathrm{c}}{\mathrm{d}t} = X - A_{m1}m_1 n_\mathrm{c} - A_{m2}m_2 n_\mathrm{c} - A_n(N - n)n_\mathrm{c}, \tag{4}$$

$$\frac{\mathrm{d}n_\mathrm{v}}{\mathrm{d}t} = X - B_2(M_2 - m_2)n_\mathrm{v} - B_1(M_1 - m_1)n_\mathrm{v}. \tag{5}$$

Here, $M_2\,(\mathrm{m}^{-3})$ is the concentration of the radiative hole centers with instantaneous occupancy of $m_2\,(\mathrm{m}^{-3})$, $M_1\,(\mathrm{m}^{-3})$ is the concentration of nonradiative hole centers with instantaneous occupancy of $m_1\,(\mathrm{m}^{-3})$, $N\,(\mathrm{m}^{-3})$ is the concentration of the electron trapping state with instantaneous occupancy of $n\,(\mathrm{m}^{-3})$. n_c and n_v are the concentrations (m^{-3}) of electrons and holes in the conduction and valence bands, respectively. X $(\mathrm{m}^{-3}\mathrm{s}^{-1})$ is the rate of production of electron–hole pairs, which is proportional to the excitation dose rate, B_1 and B_2 $(\mathrm{m}^3\mathrm{s}^{-1})$ are the trapping coefficients of free holes in centers 1 and 2, respectively. A_{m1} and A_{m2} $(\mathrm{m}^3\mathrm{s}^{-1})$ are the recombination coefficients for free electrons with holes in centers 1 and 2 and A_n $(\mathrm{m}^3\mathrm{s}^{-1})$ is the retrapping coefficient of free electrons into the trapping state N. It should be noted that in some instances, the occurrence of a competing trapping state is of importance with regard to the nonmonotonic dose dependence, in which case, Eq. (3) is replaced by two similar equations, one with n_1, N_1 and A_{n1} and the other with n_2, N_2 and A_{n2}, namely,

$$\frac{\mathrm{d}n_1}{\mathrm{d}t} = A_{n1}(N_1 - n_1)n_\mathrm{c}, \tag{3a}$$

$$\frac{\mathrm{d}n_2}{\mathrm{d}t} = A_{n2}(N_2 - n_2)n_\mathrm{c}. \tag{3b}$$

A_{n1}, N_1 and n_1 replace A_n, N, and n in Eq. (4) and the term $-A_{n2}(N_2 - n_2)n_\mathrm{c}$ must be added. The set of 6 simultaneous
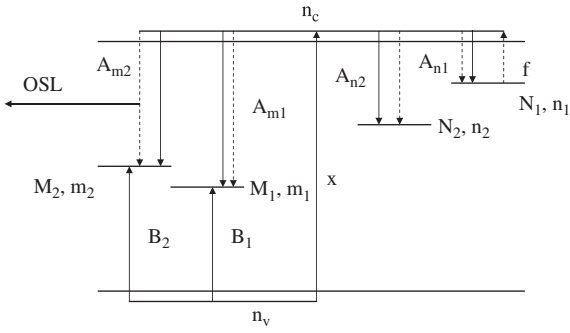
Fig. 1. The energy level diagram of two trapping levels and two kinds of recombination centers. Transitions occurring during excitation are given by solid lines, and transitions taking place during the readout stage are shown by dashed lines.

equations should be solved for the excitation stage. If we denote the time of excitation by t_D, $D = Xt_D$ is the total concentration per unit volume of electrons and holes produced, which is proportional to the total dose imparted. It should be mentioned that at the end of the excitation, free electrons and holes remain in the conduction and valence bands, respectively. In order to simulate the experimental situation properly, one has to consider a relaxation time following the excitation and prior to the heating stage, during which practically all the free carriers relax and end up in the traps and centers. It should be noted that the relaxation process is important because the carriers can build up to significant levels during excitation, and relaxation is needed to provide the time necessary for them to decay back toward zero.

All this is identical to the previously described (see Chen et al., 2006) situation concerning TL. As for the readout stage, the situation is somewhat different than in TL. The set of equations to be solved here is

$$\frac{dn_1}{dt} = -fn_1 + A_{n1}(N_1 - n_1)n_c, \tag{6}$$

$$\frac{dn_2}{dt} = A_{n2}(N_2 - n_2)n_c, \tag{7}$$

$$\frac{dm_1}{dt} = -A_{m1}m_1n_c, \tag{8}$$

$$\frac{dm_2}{dt} = -A_{m2}m_2n_c, \tag{9}$$

$$\frac{dn_1}{dt} + \frac{dn_2}{dt} + \frac{dn_c}{dt} = \frac{dm_1}{dt} + \frac{dm_2}{dt}. \tag{10}$$

Here, $f(s^{-1})$ is a magnitude proportional to the stimulating light intensity. The model assumes that the stimulating light does not raise electrons from the competing trap N_2. Obviously, in the "reduced" model with one trapping state, Eq. (7) is disregarded and we can denote N_1 by N. The OSL intensity is associated with the recombination into m_2, therefore the intensity $I(t)$ is

$$I(t) = A_{m2}m_2n_c. \tag{11}$$

It should be noted that whereas in the work on TL, the maximum intensity was usually taken as the TL signal, here we prefer to follow the experimental practice in which one usually considers the integral over the decaying OSL curve over a certain period of time. The time interval chosen for integration along the OSL decay curve depends on the dose given to the sample. In general, during the simulation this time interval is chosen long enough to deplete the trap concentrations to zero.

3. Numerical results

The matlab odes23 solver was used to solve numerically the relevant sets of equations, as well as the Mathematica solver; the results reached by these parallel ways were in excellent agreement. Eqs. (1)–(5) were first solved for a certain value of the dose rate X and for a certain length of the excitation time t_D, which together determine the dose $D = Xt_D$. The solution of the same set of equations, but with $X = 0$, is continued for a further period of relaxation time. Finally, the coupled equations for the stimulation stage, (6)–(10) were solved and Eq. (9) gave the OSL intensity as a function of time.

We have simulated the case of a model with one trapping level and two kinds of recombination centers. The parameters chosen are identical to the ones used previously to demonstrate the nonmonotonic effect in TL caused by competition during excitation (Lawless et al., 2005, Fig. 2). The values are: $M_1 = 3 \times 10^{21}\,\mathrm{m}^{-3}$, $M_2 = 1 \times 10^{18}\,\mathrm{m}^{-3}$, $A_{m1} = 1 \times 10^{-17}\,\mathrm{m}^3\,\mathrm{s}^{-1}$, $A_{m2} = 1 \times 10^{-16}\,\mathrm{m}^3\,\mathrm{s}^{-1}$, $A_n = 3 \times 10^{-17}\,\mathrm{m}^3\,\mathrm{s}^{-1}$; $E = 1.0\,\mathrm{eV}$, $s = 1 \times 10^{12}\,\mathrm{s}^{-1}$, $N = 1 \times 10^{21}\,\mathrm{m}^{-3}$, $B_1 = 1.5 \times 10^{-17}\,\mathrm{m}^3\,\mathrm{s}^{-1}$, and $B_2 = 10^{-17}\,\mathrm{m}^3\,\mathrm{s}^{-1}$. The OSL excitation rate is taken to be $f = 1\,\mathrm{s}^{-1}$. The results of the stimulation are not shown here, but they show an increase of the integrated OSL intensity with the dose up to a maximum, followed by a decrease of $\sim 35\%$ after which the integrated OSL intensity levels off at higher doses. Similar behavior is seen in the dose dependence of m_2, the radiative center occupancy at the end of the relaxation period as a function of the dose.

In Fig. 2, we show an example of nonmonotonic dose dependence governed mainly by competition during optical stimulation. The model involves two electron-trapping states and two kinds of recombination centers as shown in Fig. 1, and the trapping parameters are identical to the parameters in Lawless et al. (2005), Fig. 3. They are: $M_1 = 3 \times 10^{21}\,\mathrm{m}^{-3}$, $M_2 = 1 \times 10^{18}\,\mathrm{m}^{-3}$, $A_{n1} = 3 \times 10^{-20}\,\mathrm{m}^3\,\mathrm{s}^{-1}$, $E_1 = 1.0\,\mathrm{eV}$, $A_{n2} = 3 \times 10^{-17}\,\mathrm{m}^3\,\mathrm{s}^{-1}$, $E_2 = 1.8\,\mathrm{eV}$, $s_1 = 1 \times 10^{12}\,\mathrm{s}^{-1}$, $s_2 = 1 \times 10^{10}\,\mathrm{s}^{-1}$, $A_{m1} = 1 \times 10^{-17}\,\mathrm{m}^3\,\mathrm{s}^{-1}$, $A_{m2} = 1 \times 10^{-18}\,\mathrm{m}^3\,\mathrm{s}^{-1}$, $B_1 = 1.5 \times 10^{-19}\,\mathrm{m}^3\,\mathrm{s}^{-1}$, $B_2 = 1 \times 10^{-17}\,\mathrm{m}^3\,\mathrm{s}^{-1}$, $N_1 = 1 \times 10^{19}\,\mathrm{m}^{-3}$, and $N_2 = 1 \times 10^{21}\,\mathrm{m}^{-3}$. The solid line shows the dependence of the integrated OSL signal on the excitation dose. The curve reaches a maximum and decreases at higher doses. As opposed to the previous case, this does not reflect the behavior of the occupancy of the radiative center, m_2 shown by the dotted line. The dependence of the ratio m_2/m_1 is depicted by the dashed line, which reaches a maximum at the same dose as the OSL nonmonotonic peak shape and declines at higher doses.

At high doses, our simulation results show that m_1 and n_2 continue to increase while n_1 and m_2 approach constant values.
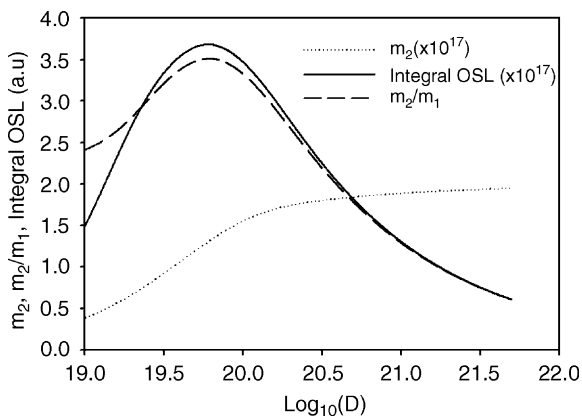
Fig. 2. Simulated dose dependence of integrated OSL intensity (solid line), the radiative center concentration following irradiation and relaxation, m_2, and the ratio of radiative to nonradiative centers, m_2/m_1, when competition during readout dominates. The relevant set of parameters is given in the text.

Fig. 4. Simulated dose dependence of integrated OSL intensity (solid line) and of the radiative center concentration following irradiation and relaxation, m_2. The relevant set of parameters is given in the text.
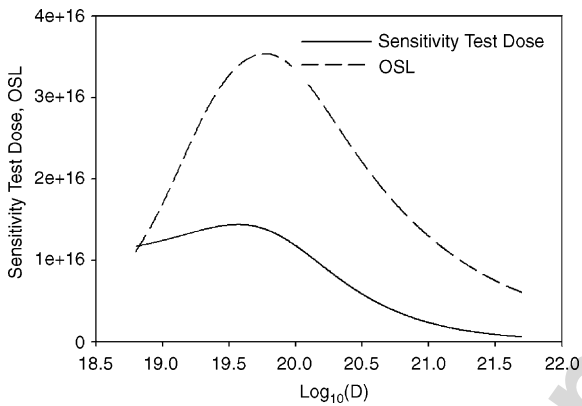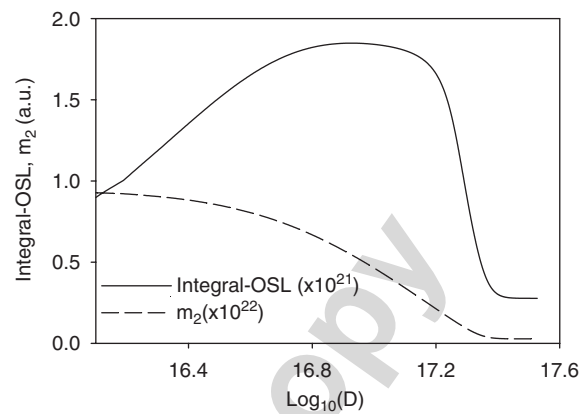

Fig. 3. Simulated dose dependence of OSL sensitivity to small β test dose, using the same parameters as in Fig. 2.

These larger values of m_1 create more competition for the radiative center m_2 and cause OSL to continue to decline. Note that n_2 plays an important role here: by conservation of charge, and with n_1 and m_2 roughly constant, m_1 could not continue to increase without n_2 increasing by the same amount. This cannot take place when N_2 is relatively small. In fact, if we set $N_2 = 0$ while keeping the other parameters the same, the simulation results show that the nonmonotonic effect disappears.

It is noted that not all 2 trap-2 center sets of parameters will yield this behavior. This is merely a demonstration that such nonmonotonic dose dependence is possible. The behavior seen is the result of the choice of all 10 relevant parameters (M_1, M_2, N_1, N_2, B_1, B_2, A_{m1}, A_{m2}, A_{n1}, A_{n2}). In fact, giving an intuitive argument is more complicated since one has to consider the role of each of the 10 parameters both during excitation and readout. The qualitative arguments given here relate only to the obvious connection between the ratio m_2/m_1 and the OSL signal in the given results.

Of special interest to researchers in both dating and retrospective dosimetry is the change of sensitivity of quartz samples to a small β test dose, after repeated irradiations of the same

aliquot. For the case shown in Fig. 2, we may expect a change in the sensitivity after the sample has received large irradiations, since some hole populations will be retained in M_1 and also perhaps M_2, resulting in m_{20} and m_{10} not being equal to zero. We have investigated this experimental situation by simulating the following series of steps: (a) the sample is given a small β test dose (corresponding to the smallest dose shown in Fig. 2), and the OSL signal is measured, (b) the same sample is given a large β dose and the OSL signal is measured. This step produces the OSL signal shown in Fig. 2. (c) the same sample is again given the same test dose and the new sensitivity is measured once more. The results of simulating these steps are shown in Fig. 3, where the sensitivity is found to follow nonmonotonic dose dependence similar to that of the integrated OSL signal. Specifically, the sensitivity to the test dose is seen to increase with dose, reach a maximum value $\sim 30\%$ higher than the starting value, and then decreases continuously with the β dose, approaching zero at very large doses. The behavior of the OSL sensitivity with the β dose is similar to the experimental data in Yukihara et al. (2004a, b), Fig. 5b.

A different kind of nonmonotonic dose dependence is shown in Fig. 4. The model includes two trapping states and two kinds of recombination centers and may explain several experimental results for the important dosimetric material Al_2O_3:C (Yukihara et al., 2004a, b). Yukihara et al. (2003, 2004a) studied in detail three Al_2O_3:C samples from different batches labeled D320, Chip101 and B1040. Yukihara et al. (2003) carried out a comprehensive experimental study of the effect of deep traps on the TL of Al_2O_3:C by using both β irradiation and UV illumination, as well as by employing step-annealing techniques. The concentration of F and F^+ centers in the samples were monitored by optical absorption measurements, and competing deep hole and deep electron traps were identified. Yukihara et al. (2003) concluded that their experimental data were consistent with a model consisting of two traps and two centers. In the model presented here, the total concentrations are denoted by N_1 for the dosimetric trap, by N_2 for the competing deep electron trap, by M_2 for the radiative

F^+ centers and by M_1 for the competing nonradiative deep hole center.

The model presented here reproduces the main features of the experimental TL and OSL vs. β dose behavior, including the nonmonotonic behavior at high doses. A representative set of parameters used here are: $M_1 = 2.4 \times 10^{22}$ m^{-3}, $M_2 = 10^{23}$ m^{-3}, $A_{n1} = 2 \times 10^{-14}$ m^3 s^{-1}, $A_{n2} = 2 \times 10^{-15}$ m^3 s^{-1}, $E_1 = 1.3$ eV, $s_1 = 1 \times 10^{13}$ s^{-1}; $A_{m1} = 5 \times 10^{-17}$ m^3 s^{-1}, $A_{m2} = 4 \times 10^{-14}$ m^3 s^{-1}, $B_1 = 4 \times 10^{-15}$ m^3 s^{-1}, $B_2 = 10^{-14}$ m^3 s^{-1}, $N_1 = 2 \times 10^{21}$ m^{-3} and $N_2 = 2 \times 10^{21}$ m^{-3}. The initial concentrations of electrons and holes in the model are taken as $n_c = n_v = n_1 = n_2 = m_2 = 0$ and the initial concentration of the luminescence center is taken as $m_{20} = 9.43 \times 10^{21}$ m^{-3}.

Appendix A is a detailed series of reasonable physical assumptions which leads to an estimate of the kinetic parameters for the model. Some of the arguments are based on the experimental data of Yukihara et al. (2003), while other parameters are taken to represent "typical values" as reported in the literature for a variety of materials. Furthermore, an estimate is obtained for the conversion factor between the experimentally measured dose rate (in Gy/sec), and the excitation rate X (in electron–hole pairs per cm^3 per s) by using the physical properties of alumina.

The calculated graphs of OSL versus dose and m_2 versus dose shown in Fig. 4 are qualitatively very similar to the published data for samples D320 and Chip101 in Fig. 8 by Yukihara et al. (2003) and in Fig. 1 of Yukihara et al. (2004a).

The physical basis of this nonmonotonic effect in alumina is rather complex, and only a simplified version can be given here, as follows. After irradiation and relaxation ($n_c = n_v = 0$), the condition $m_2 = n_1 + n_2 + m_2(0) - m_1$ will be satisfied. In samples D320 or Chip 101, it is observed that ($n_1 + n_2$) initially grows with dose about as fast as m_1. However, as n_1 begins to saturate, the growth of ($n_1 + n_2$) with dose slows down while m_1 continues to grow faster than ($n_1 + n_2$). Consequently, the radiative center, m_2, declines in this dose range and this causes the observed decline in luminescence.

Looked at in more mechanistic detail, as n_1 begins to saturate, a larger fraction of the electrons produced by the irradiation recombine with the centers or more specifically recombine with m_2 because we have assumed $A_{m1} \ll A_{m2}$. At this point the recombination of m_2 with electrons becomes faster than the capture of holes into m_2 and causes the decline in m_2. In Lawless et al. (2005), we demonstrated the nonmonotonic effect in a case with a "small" radiative center, M_2, and a "large" nonradiative center, M_1, while the initial concentration $m_2(0)$ was zero. The case herein extends this previous situation, to demonstrate that a nonmonotonic effect is possible with non-zero initial m_2 and with a value of M_2 of comparable or larger size as M_1, provided that $A_{m1} \ll A_{m2}$.

We have also modelled the case where the detrapping probability for N_2 is 2 orders of magnitude smaller than the detrapping probability for N_1, as is observed for the slow component of quartz. The results of this simulation show that the OSL signal still displays the same nonmonotonic behavior shown in Fig. 4, but the overall OSL signal is increased by $\sim 28\%$ of the original OSL signal. This increase of the OSL signal at all

doses is most probably due to the additional electrons available from trap n_2 during the OSL excitation stage.

4. Conclusion

This paper extends the previous work of Lawless et al. (2005) to explain the nonmonotonic dose dependence of OSL.

A distinction is made between two cases. In one, the competition during excitation causes the filling of the relevant radiative center to be nonmonotonic with the dose, and as a result, the OSL intensity behaves in a similar way. This can take place with a model including one trapping state and two kinds of recombination centers, one radiative and the other nonradiative. In the other case, the nonmonotonic dose dependence of the OSL signal is mainly due to competition in the readout stage. In this case, it appears that nonmonotonic dose dependence is possible in a system with two trapping states and two kinds of recombination centers. A specific model which may be applicable to the nonmonotonic OSL and TL effect in Al$_2$O$_3$:C is also presented.

Appendix A

A.1. Arguments for the choices of the kinetic parameter

Our goal in this section is to arrive at an initial estimate of "good parameters" which can qualitatively describe the behavior of the TL and OSL vs. dose, as well as the behavior of the F$^+$ concentration (m_2) vs. β dose published by Yukihara et al. (2003).

(a) M_2 value: (Yukihara et al., 2003. p. 627) gives values of $M_2 \sim 10^{22}$–10^{23} m^{-3}. We chose the high value in this range.

(b) N_1, N_2 values: From Fig. 8 of Yukihara et al. (2003), there is no evidence of m_2 saturating ($m_2 \ll M_2$), while their data in Fig. 2 shows that dosimetric trap and the competitor electron trap (n_1 and n_2) saturate, so we can therefore assume that $N_1 \ll M_2$ and $N_2 \ll M_2$. Let us choose a typical value of $N_1 \sim 10^{21}$ m^{-3}.

By using the annealing curves in Figs. 8 and 9 in Yukihara et al. (2003) we can conclude that $N_1 \sim N_2$ as follows. The annealings were reportedly done following high dose, which results in the traps being filled. Around 450 K, the annealing curves show a decrease in m_2 as N_1 (the "dosimetric" electron trap) empties, while at around 1150 K they show a further decrease in m_2 as N_2 (the "deep" electron traps) empty. Since the decreases in m_2 look comparable in magnitude, we can assume that $N_1 \sim N_2$ as a first approximation.

(c) A_{n1}, A_{n2}, A_{m1}, A_{m2} values: Suppose A_{n1} is in the "typical" range of capturing cross-sections as reported for a wide variety of materials (Rose, 1955; Lax, 1960): $A_{n1} \sim 10^{-14}$ m^3 s^{-1}. From the experimental data of Fig. 2a in Yukihara et al. (2003), the dosimetric trap (n_1) saturates first at ~ 25 Gy, while the deep electron trap (n_2) shows an experimental saturation dose of ~ 150 Gy, so we can choose $A_{n2} \sim 2 \times 10^{-15}$ m^3 s^{-1}. We also choose the value of the recombination coefficient A_{m2} to be in the "typical" range:

$A_{m2} \sim 2 \times 10^{-14}\,\text{m}^3\,\text{s}^{-1}$. The value of A_{m1} is chosen much smaller than A_{m2}, so that the deep hole trap M_1 is a rather weak competitor for the electrons in the conduction band: $A_{m1} \sim 5 \times 10^{-17}\,\text{m}^3\,\text{s}^{-1}$.

(d) M_1 value: From Fig. 2a of Yukihara et al. (2003), it appears that a dose of 200 Gy was enough to saturate n_1, n_2 and m_1. By conservation of charge (after relaxation), $m_1 + m_2 = n_1 + n_2$. If n_1, n_2 and m_1 are saturated at 200 Gy, then $M_1 + m_2 = N_1 + N_2$. From Fig. 8a of Yukihara et al. (2003), it appears that the three materials have small values of m_2 at 200 Gy. Therefore, at a dose of ~ 200 Gy we may approximate $M_1 \sim N_1 + N_2 : M_1 \sim N_1 + N_2 \sim 2 \times 10^{21}\,\text{m}^{-3}$. The final adjusted values for this parameter in the model is an order of magnitude larger, $M_1 = 2.4 \times 10^{22}\,\text{m}^{-3}$. It was found necessary to increase this value in order to obtain better agreement with the experimental data of Yukihara et al. (2003).

(e) B_1, B_2, m_{20} values: As discussed in the next section, by assuming that $B_1 \sim B_2$ and by using the estimated values of $A_{m2}, A_{n1}, A_{n2}, N_1, N_2, M_1$ and M_2, we can estimate the initial population of the recombination centers m_{20}. $m_{20} \sim 10^{21}$–$10^{22}\,\text{m}^{-3}$. As a starting value of B_1, B_2 we choose $B_1 \sim B_2 = 10^{-14}\,\text{m}^3\,\text{s}^{-1}$ (as a "typical value"). The final adjusted values for these two parameters in the model are $B_1 = 4 \times 10^{-15}\,\text{m}^3\,\text{s}^{-1}$; $B_2 = 10^{-14}\,\text{m}^3\,\text{s}^{-1}$.

A.2. Derivation of the mathematical condition for Center population vs. dose

In the two-electron trap and two hole–center model presented in the text, free electrons are created at a rate of X. These free electrons are captured either by the dosimetric trap (n_1), by the competing trap (n_2), or by the recombination center (m_2) because A_{m1} is negligible. The fraction of the electrons going into m_2 is

$$\frac{A_{m2}m_2}{A_{m2}m_2 + A_{n1}(N_1 - n_1) + A_{n2}(N_2 - n_2)}. \tag{12}$$

Similarly, the rate at which free holes are created is X, and these holes are either captured by m_1 or by m_2. The fraction captured by m_2 is

$$\frac{B_2(M_2 - m_2)}{B_1(M_1 - m_1) + B_2(M_2 - m_2)}. \tag{13}$$

The center population m_2 will remain unchanged with increasing dose if its electron capture rate is the same as its hole capture rate, i.e. $\mathrm{d}m_2/\mathrm{d}t = 0$:

$$\frac{A_{m2}m_2}{A_{m2}m_2 + A_{n1}(N_1 - n_1) + A_{n2}(N_2 - n_2)}
= \frac{B_2(M_2 - m_2)}{B_1(M_1 - m_1) + B_2(M_2 - m_2)}. \tag{14}$$

The above can be readily simplified, yielding

$$\frac{A_{m2}m_2}{A_{n1}(N_1 - n_1) + A_{n2}(N_2 - n_2)} = \frac{B_2(M_2 - m_2)}{B_1(M_1 - m_1)}. \tag{15}$$

Before irradiation, we can assume that the electron and hole traps are empty: $n_{10} = n_{20} = m_{10} = 0$. Therefore, the above condition reduces to

$$\frac{A_{m2}m_{20}}{A_{n1}N_1 + A_{n2}N_2} = \frac{B_2 M_2}{B_1 M_1}. \tag{16}$$

This equation is used to obtain an initial estimate of the initial recombination center population m_{20} for the simulation. By assuming that $B_1 \sim B_2$ and by using the estimated values of $A_{m2}, A_{n1}, A_{n2}, N_1, N_2, M_1$ and M_2 from the previous section, we can estimate the initial population of the recombination centers m_{20} by using Eq. (16): $m_{20} \sim 10^{21}$–$10^{22}\,\text{m}^{-3}$.

A.3. Relating the excitation rate X to the actual dose D in Gy

If the material is subjected to a dose D in Gy over a period of t seconds, then the excitation rate X is

$$X = \frac{\rho D}{Wt}, \tag{17}$$

where ρ is the mass density and W is the energy deposited per electron–hole pair created. In the gas phase, W is well-characterized and typically $\sim 2.2 \times E_I$ where E_I is the ionization potential. For every amount W of energy deposited, an amount E_I ends up in ionization and the remaining energy, $1.2E_I$, ends up in excited states and heat. In solids, the minimum possible value of W is the band gap: $W = E_g$.

Let us consider a 1-s long 1-Gy dose in alumina. For alumina, $E_g = 9.8\,\text{eV}$ and $\rho = 4\,\text{g}\,\text{cm}^{-3}$. The energy W can be treated as an adjustable parameter in the model, with its value adjustable to give the best possible fit to the experimental data of Yukihara et al. (2004a), so we choose $W = 1.5E_g$. Then for $D = 1$ Gy and $t = 1$ s, and using the definition $1\,\text{Gy} = 1\,\text{Joule/kg}$, the above equation gives

$$X = \frac{\rho D}{WT} = 1.7 \times 10^{15} \text{ electron–hole pairs per cm}^3 \text{ per s}. \tag{18}$$

References

Bloom, D., Evans, D.R., Holmstrom, S.A., Polf, J.C., McKeever, S.W.S., Whitley, V., 2003. Characterization of Al$_2$O$_3$ single crystals by the laser-heated pedestal growth technique for potential use in radiation dosimetry. Radiat. Meas. 37, 141–149.

Böhm, M., Pitt, E., Scharmann, A., 1984. Uncommon TLD materials. Radiat. Prot. Dosim. 8, 139–143.

Chen, R., Lo, D., Lawless, J.L., 2006. Non-monotonic dose dependence of thermoluminescence. Radiat. Prot. Dosim., in press.

Freytag, E., 1971. Measurement of high doses with glass dosemeters. Health Phys. 20, 93–94.

Lawless, J.L., Chen, R., Lo, D., Pagonis, V., 2005. A model for non-monotonic dose dependence of thermoluminescence (TL). J. Phys. Condens. Matter 17, 737–753.

Lax, M., 1960. Cascade capture of electrons in solids. Phys. Rev. 119, 1502–1523.

Rose, A., 1955. Recombination processes in insulators and semiconductors. Phys. Rev. 97, 322–333.

Schulman, J.H., Etzel, H.W., Allard, J.G., 1957. Application of luminescence changes in organic solids to dosimetry. J. Appl. Phys. 28, 792–795.

Tesch, K., 1983. Measurement of doses between 10^{-2} and 10^8 Gy with glass dosemeters. Radiat. Prot. Dosim. 6, 347–349.

Yukihara, E.G., Whitley, V.H., Polf, J.C., Klein, D.M., McKeever, S.W.S., Akselrod, A.E., Akselrod, M.S., 2003. The effects of deep trap population on the thermoluminescence of Al_2O_3:C. Radiat. Meas. 37, 627–638.

Yukihara, E.G., Whitley, V.H., McKeever, S.W.S., Akselrod, A.E., Akselrod, M.S., 2004a. Effect of high-dose irradiation on the optically stimulated luminescence of Al_2O_3:C. Radiat. Meas. 38, 317–330.

Yukihara, E.G., Gaza, R., McKeever, S.W.S., Soares, C.G., 2004b. Optically stimulated luminescence and thermoluminescence efficiencies for high-energy heavy charged particle irradiation in Al_2O_3:C. Radiat. Meas. 38, 59–70.

Zeneli, D., Tavlet, M., Coninckx, F., 1996. Response of radio-photoluminescence dosemeters irradiated at cryogenic temperatures. Radiat. Prot. Dosim. 66, 205–207.